Pergamon

Int. J. Solids Structures Vol. 34, No. 19, pp. 2497–2516, 1997

0020–7683/97 $17.00 + .00

PII: S0020–7683(96)00115–1

FINITE ELEMENT SOLUTION OF THE STABILITY PROBLEM FOR NONLINEAR UNDAMPED AND DAMPED SYSTEMS UNDER NONCONSERVATIVE LOADING

RENATO V. VITALIANI and ALESSANDRO M. GASPARINI
Dipartimento di Costruzioni e Trasporti, Università di Padova, Via Marzolo 9, Padova, 35131, Italy

and

ANNA V. SAETTA
Dipartimento di Costruzione dell'Architettura, Istituto Universitaio di Architettura di Venezia, Tolentini 191, Venezia, 30135, Italy

(*Received* 17 *April* 1995; *in revised form* 30 *May* 1996)

Abstract—A nonlinear finite element analysis of elastic structures which can be studied by a 3D beam theory, subjected to conservative as well as to nonconservative forces, is presented. The stability behaviour of the system is studied by means of an eigenvalue analysis. The stiffness matrix of the eigenvalue problem is asymmetric (i.e., non-self-adjoint system). The flutter and divergence modes of instability, as well as the values of the critical load, are identified for a number of numerical examples belonging to the benchmark tests proposed by NAFEMS (1990). The results demonstrate the reliability of this finite element formulation. In particular the effect of damping on the stability behaviour of such structures is investigated and the destabilizing effect of small damping is underlined. Finally, the need to define a number of benchmark tests for nonlinear–nonconservative analyses in presence of damping is included. © 1997 Elsevier Science Ltd.

1. INTRODUCTION

A large number of theoretical studies, as well as numerical simulation using finite elements, to solve geometrically nonlinear problems of elastic beams can be found in more and less recent works of many authors (e.g., Argyris *et al.*, 1981a, 1981b, 1982; Alliney and Tralli, 1984; Surana and Sorem, 1989; Simo and Vu-Quoc, 1986, 1988, 1991). Moreover, a lot of formulations can be found in literature to accommodate large rotation capability during deformation process, e.g., by using Euler angles, Euler parameters, Milenkovic or Rodriges parameters, or the Simo approach.

This paper develops a geometrically nonlinear finite element analysis of elastic structures subjected to both conservative and nonconservative forces, using the Total Lagrangian approach. The basic curved beam geometry and configuration here adopted are those developed by one of the authors in Martini and Vitaliani (1988), while the element displacement field approximation is expressed in terms of the three nodal translations and nonlinear function of the three nodal rotations, according to the hypothesis assumed by Surana and Sorem (1989).

In this study, interest is restricted to small strain, finite rotation, finite displacement behaviour of structures, which can be idealised as assemblages of 3D beams, and particular attention is focused on the stability behaviour of such systems under nonconservative loads.

The stability of nonconservative systems has been extensively studied [see, e.g., Bolotin (1965) and Ziegler (1968)]. The presence of nonconservative loads makes the equation system mathematically non-self-adjoint and the corresponding eigenvalue problem is ruled by a non-symmetric matrix and can exhibit complex eigenvalues. A comprehensive discussion of the dynamic stability subject, with a related list of references until 1990, can be found, for example, in the book by El Naschie (1990).

The stability behaviour of nonconservative systems can be studied with two different approaches, respectively: the global and the local stability analysis. The use of a complete nonlinear dynamic analysis allows to establish the global divergence as well as the global oscillatory stability (i.e., the long term stability), while a static nonlinear analysis associated with the examination of the nature of the eigenvalues in the neighbourhood of the current equilibrium solution, can be adopted to study the loss of local stability, both via divergence or via flutter [Kounadis (1991), Kounadis and Avraam (1991), Krätzig *et al.* (1991), Kounadis and Smitses (1993), Thomsen (1993), Kounadis (1994)].

This second approach is far more economical compared with the complete nonlinear dynamic one, and it provides all the information required to calculate the critical value of the load, both with and without damping effect, and to specify the actual boundaries of the stability and instability regions, e.g., Gasparini *et al.* (1995). Moreover, the results obtained with such a procedure can be used as preliminary analysis to identify the regions where the full nonlinear dynamic method is actually needed. However, it is worth noting that the complete nonlinear dynamic method is imperative for analyzing post-critical behaviour as well as for establishing whether a region is of flutter instability (oscillation with increasing amplitudes) or if there is a periodic motion (bounded amplitude motions) (Kounadis, 1991 and 1994).

In the finite element formulation, the study of geometrically nonlinear elastic systems under nonconservative loads, produces a non-symmetric total tangent stiffness matrix, due to the contribution of the load correction matrix. For more efficient numerical analysis, this contribution is sometimes neglected, but this can be accepted only for a certain class of structures, i.e., for systems which lose stability always via divergence.

In all the numerical examples presented in this work, the full nonsymmetric load correction matrix is considered, so allowing to study both the divergence and the flutter mode of instability.

Some benchmark problems drawn from the NAFEMS (1990) are solved ratifying the correctness and the efficiency of the proposed procedure. All the examples shown the same results published by the NAFEMS, except for the case of a right angled frame under end load (test B18). For this test some more information is supplied, in order to explain its particular behaviour, principally in presence of damping.

In fact, as known, a more precise modelling of real structures needs to take the damping effect into consideration. This implies the treatment of a quadratic eigenvalue problem in order to establish the stability condition of the current equilibrium configuration. In this work the effect of a damping ratio variable from almost zero value to a typical value is evaluated for all the proposed numerical examples that show flutter instability (i.e., the divergence systems are not influenced by the presence of damping), and the destabilizing effect of small damping is emphasised (Kounadis, 1992 and 1994; Bratus, 1993).

The necessity and the importance of considering the presence of damping in the evaluation of the critical load of nonlinear systems subjected to nonconservative loads, requires the definition of benchmark problems to test the procedures and the finite element formulations also for the damped stability analysis, with variable damping ratio. This could be done starting from the results reported in this paper, that concern only the condition of uniformly distributed Rayleigh-damping.

2. BEAM ELEMENT APPROXIMATION

2.1. *Geometrical description and local axes definition*

Let us consider a curved and twisted beam in a fixed coordinate system X, Y, Z (Fig. 1). An orthogonal curvilinear coordinate system is introduced to describe the motion of the beam. The local axes are defined according to Martini and Vitaliani (1988) by the unit vectors **t**, **n**, and **b**, which are, respectively, tangential, normal and binormal of the skew axis of the beam on point P. As it is known from differential geometry, the normal **n** is the unit vector perpendicular to the tangent **t** in P of the axis ξ and belonging to the osculating plane. The geometrical definitions of unit vectors such as these are the following:

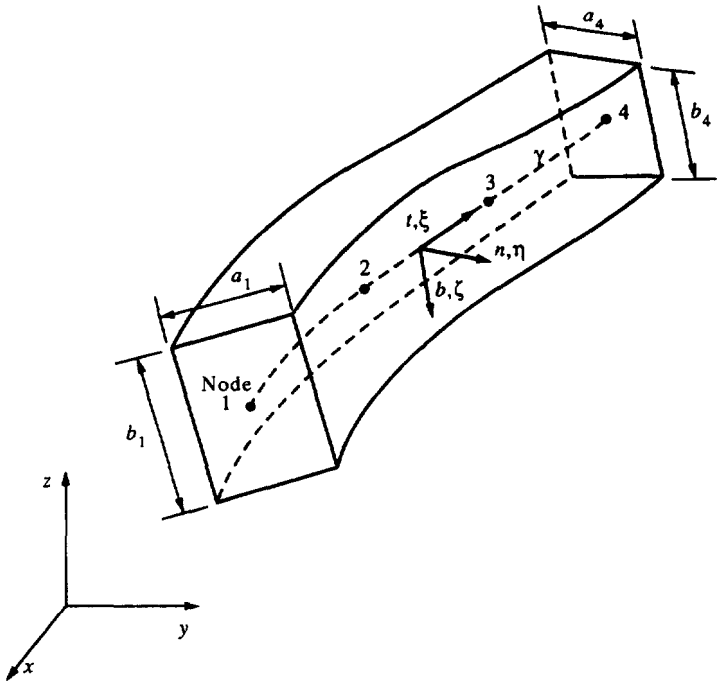

Fig. 1. Curved beam geometry and local coordinate system definition.

$$\mathbf{t} = \frac{\dfrac{\mathrm{d}\mathbf{P}}{\mathrm{d}t}}{\left|\dfrac{\mathrm{d}P}{\mathrm{d}t}\right|} = \frac{\dfrac{\mathrm{d}\mathbf{P}}{\mathrm{d}t}}{\left|\dfrac{\mathrm{d}s}{\mathrm{d}t}\right|} = \frac{\mathrm{d}\mathbf{P}}{\mathrm{d}s}$$

$$\mathbf{n} = \frac{\dfrac{\mathrm{d}\mathbf{t}}{\mathrm{d}t}}{\left|\dfrac{\mathrm{d}\mathbf{t}}{\mathrm{d}s}\right|} = \rho\frac{\mathrm{d}\mathbf{t}}{\mathrm{d}s}$$

$$\mathbf{b} = \mathbf{t} \times \mathbf{n} \tag{1}$$

where s is the curvilinear coordinate and ρ is the curvature radius. For a skew line we have to define also the radius of torsion τ as (e.g., Vaccaro, 1968):

$$\frac{1}{\tau} = \frac{\mathrm{d}\mathbf{b}}{\mathrm{d}s} \cdot \mathbf{n}. \tag{2}$$

The transformation of coordinates from the local system ξ, η, ζ to the global system (X, Y, Z) is ruled by the transformation matrix $\mathbf{T}$ and can be written as:

$$\begin{Bmatrix} X \\ Y \\ Z \end{Bmatrix} = \begin{bmatrix} t_{t_X} & t_{n_X} & t_{b_X} \\ t_{t_Y} & t_{n_Y} & t_{b_Y} \\ t_{t_Z} & t_{n_Z} & t_{b_Z} \end{bmatrix} \begin{Bmatrix} \xi \\ \eta \\ \zeta \end{Bmatrix} \tag{3}$$

where:

$$\mathbf{T} = \{\mathbf{t} \quad \mathbf{n} \quad \mathbf{b}\} = \begin{Bmatrix} t_{t_X} & t_{n_X} & t_{b_X} \\ t_{t_Y} & t_{n_Y} & t_{b_Y} \\ t_{t_Z} & t_{n_Z} & t_{b_Z} \end{Bmatrix}.$$

For the detailed expression of terms of matrix **T** see Martini and Vitaliani (1988). The local coordinates to a point P belonging to the element section of the skew beam can be written as:

$$P \equiv \left(\xi = 0; \quad \eta \frac{a_\eta}{2}; \quad \zeta \frac{b_\zeta}{2}\right); \tag{4}$$

then the global coordinates of the point P can be expressed as functions of the position of the axis point $P_0 \equiv (X_0, Y_0, Z_0)$ of the considered cross section:

$$\begin{aligned} X &= X_0 + \frac{a_\eta}{2}\eta t_{n_X} + \frac{b_\zeta}{2}\zeta t_{b_X} \\ Y &= Y_0 + \frac{a_\eta}{2}\eta t_{n_Y} + \frac{b_\zeta}{2}\zeta t_{b_Y} \\ Z &= Z_0 + \frac{a_\eta}{2}\eta t_{n_Z} + \frac{b_\zeta}{2}\zeta t_{b_Z} \end{aligned} \tag{5}$$

where

$$X_0 = X_0(\xi) \quad Y_0 = Y_0(\xi) \quad Z_0 = Z_0(\xi) \tag{6}$$

are the parametric equations of the skew line γ, on which the axis of the element lies.

For an n-node isoparametric element, the eqns (6) can be obtained by interpolation from their nodal values and eqns (5) become:

$$\begin{aligned} X &= \sum_{i=1}^{n} N_i X_i^e + \frac{a_\eta}{2}\eta t_{n_X} + \frac{b_\zeta}{2}\zeta t_{b_X} \\ Y &= \sum_{i=1}^{n} N_i Y_i^e + \frac{a_\eta}{2}\eta t_{n_Y} + \frac{b_\zeta}{2}\zeta t_{b_Y} \\ Z &= \sum_{i=1}^{n} N_i Z_i^e + \frac{a_\eta}{2}\eta t_{n_Z} + \frac{b_\zeta}{2}\zeta t_{b_Z}. \end{aligned} \tag{7}$$

As it is well known, the Jacobian matrix of the transformation is defined as:

$$[J_c] = \begin{bmatrix} \dfrac{\partial X}{\partial \xi} & \dfrac{\partial X}{\partial \eta} & \dfrac{\partial X}{\partial \zeta} \\ \dfrac{\partial Y}{\partial \xi} & \dfrac{\partial Y}{\partial \eta} & \dfrac{\partial Y}{\partial \zeta} \\ \dfrac{\partial Z}{\partial \xi} & \dfrac{\partial Z}{\partial \eta} & \dfrac{\partial Z}{\partial \zeta} \end{bmatrix}. \tag{8}$$

For the skew beam the nine components of the Jacobian matrix can be explicitly written as follows:

$$\frac{\partial X}{\partial \xi} = \sum_{i=1}^{n} \frac{\partial N_i}{\partial \xi} X_i^e + \frac{a_\eta}{2}\eta \frac{\partial t_{n_x}}{\partial \xi} + \frac{b_\zeta}{2}\zeta \frac{\partial t_{b_x}}{\partial \xi}$$

$$\frac{\partial X}{\partial \eta} = \frac{a_\eta}{2} t_{n_x}$$

$$\frac{\partial X}{\partial \zeta} = \frac{b_\zeta}{2} t_{b_x}$$

$$\frac{\partial Y}{\partial \xi} = \sum_{i=1}^{n} \frac{\partial N_i}{\partial \xi} Y_i^e + \frac{a_\eta}{2}\eta \frac{\partial t_{n_y}}{\partial \xi} + \frac{b_\zeta}{2}\zeta \frac{\partial t_{b_y}}{\partial \xi}$$

$$\frac{\partial Y}{\partial \eta} = \frac{a_\eta}{2} t_{n_y}$$

$$\frac{\partial Y}{\partial \zeta} = \frac{b_\zeta}{2} t_{b_y}$$

$$\frac{\partial Z}{\partial \xi} = \sum_{i=1}^{n} \frac{\partial N_i}{\partial \xi} Z_i^e + \frac{a_\eta}{2}\eta \frac{\partial t_{n_z}}{\partial \xi} + \frac{b_\zeta}{2}\zeta \frac{\partial t_{b_z}}{\partial \xi}$$

$$\frac{\partial Z}{\partial \eta} = \frac{a_\eta}{2} t_{n_z}$$

$$\frac{\partial Y}{\partial \zeta} = \frac{b_\zeta}{2} t_{b_z}. \tag{9}$$

Therefore, the derivative of the shape functions in the global system can be obtained by means of the Jacobian as:

$$\begin{Bmatrix} \frac{\partial N_i}{\partial X} \\ \frac{\partial N_i}{\partial X} \\ \frac{\partial N_i}{\partial X} \end{Bmatrix} = [J_c^T]^{-1} \begin{Bmatrix} \frac{\partial N_i}{\partial \xi} \\ \frac{\partial N_i}{\partial \eta} \\ \frac{\partial N_i}{\partial \zeta} \end{Bmatrix}. \tag{10}$$

In a Total Lagrangian formulation the derivatives are calculated with respect to the initial coordinate system (Bathe, 1982).

2.2. *Displacement field*

The geometry of the element, described by eqns (7), can be written in a more concise form as:

$$\begin{Bmatrix} X \\ Y \\ Z \end{Bmatrix} = \sum_{i=1}^{n} N_i(\xi) \begin{Bmatrix} X_i \\ Y_i \\ Z_i \end{Bmatrix} + \left(\frac{a_\eta}{2}\eta\right)\mathbf{n}(\xi) + \left(\frac{b_\zeta}{2}\zeta\right)\mathbf{b}(\xi). \tag{11}$$

Similarily, the displacement approximation at a point $P\ (\xi, \eta, \zeta)$ within the finite element can be written in terms of the nodal translations U_i, V_i, W_i along the global axes, and of the rotations α_i, β_i, γ_i about the local axes (Surana and Sorem, 1989) by means of the vector $\mathbf{F}_i$ and $\mathbf{G}_i$ as follows:

$$\begin{Bmatrix} U \\ V \\ W \end{Bmatrix} = \sum_{i=1}^{n} N_i(\xi) \begin{Bmatrix} U_i \\ V_i \\ W_i \end{Bmatrix} + \left(\frac{a_\eta}{2}\eta\right) \sum_{i=1}^{n} N_i(\xi)\mathbf{F}_i + \left(\frac{b_\zeta}{2}\zeta\right) \sum_{i=1}^{n} N_i(\xi)\mathbf{G}_i \tag{12}$$

where $\mathbf{F}_i = \begin{Bmatrix} F_{ix} \\ F_{iy} \\ F_{iz} \end{Bmatrix}$ and $\mathbf{G}_i = \begin{Bmatrix} G_{ix} \\ G_{iy} \\ G_{iz} \end{Bmatrix}$ are the nonlinear functions of nodal rotations and are defined in more detail in Surana and Sorem (1989).

2.3. *Element stiffness matrix*

Within a Total Lagrangian approach, the Green's strains and the Piola Kirchhoff's stresses are used in the formulation of the nonlinear 3D beam element. The classical material matrix **D** relates the strain increments to the stress increments (e.g., Zienkiewicz and Taylor, 1989; Bathe, 1982).

By using the theory of geometrically nonlinear analysis within the classical finite element method, the global stiffness matrix $\mathbf{K}_T$ of the structure can be obtained by the addition of the Cartesian elastic, the initial displacement and the initial stress stiffness matrices $\mathbf{K}^0$, $\mathbf{K}^L$ and $\mathbf{K}^S$, respectively.

Nonconservative forces of the follower type (i.e., displacement dependent) lead to non-self-adjoint boundary value problems. Within the finite element formulation, the effect of such forces is in fact to produce a non-symmetric load correction matrix $\mathbf{K}^{nc}$ which has to be added to the total tangent stiffness matrix. Therefore the global tangential matrix becomes non-symmetric and can be expressed by:

$$\mathbf{K}_T = \mathbf{K}^0 + \mathbf{K}^L + \mathbf{K}^S + \mathbf{K}^{nc}. \tag{13}$$

The load correction matrix can be defined as follows:

$$\mathbf{K}^{nc} = \frac{\partial \mathbf{P}^{nc}}{\partial \mathbf{u}} = \begin{bmatrix} \frac{\partial P_1^{nc}}{\partial u_1} & \frac{\partial P_1^{nc}}{\partial u_2} & \cdots & \cdots & \frac{\partial P_1^{nc}}{\partial u_n} \\ \frac{\partial P_2^{nc}}{\partial u_1} & \frac{\partial P_2^{nc}}{\partial u_2} & \cdots & \cdots & \frac{\partial P_2^{nc}}{\partial u_n} \\ \cdots & \cdots & \cdots & \cdots & \cdots \\ \cdots & \cdots & \cdots & \cdots & \cdots \\ \frac{\partial P_n^{nc}}{\partial u_1} & \frac{\partial P_n^{nc}}{\partial u_2} & \cdots & \cdots & \frac{\partial P_n^{nc}}{\partial u_n} \end{bmatrix} \tag{14}$$

where $\mathbf{P}^{nc}$ is the vector of kinematically equivalent nodal forces resulting from the non-conservative external loading and **u** is the generalised displacement vector.

3. THE PROBLEM OF ELASTIC STABILITY

In correspondence of an equilibrium position, the tangential equation of motion in the finite element formulation can be written as follows:

$$\mathbf{M}\ddot{\mathbf{u}} + \mathbf{C}_T\dot{\mathbf{u}} + \mathbf{K}_T\mathbf{u} = 0 \tag{15}$$

where **M**, $\mathbf{C}_T$, and $\mathbf{K}_T$ are, respectively, the global mass matrix, the tangential damping matrix and tangential stiffness matrix defined by the eqn (13), **u** is the displacement vector. By assuming $\mathbf{u} = \mathbf{u}_0 \cdot e^{\lambda t}$ as trial function, in the hypothesis that all the characteristic components of the tangential equation of motion would be time-invariant matrices, the resulting eigenvalue problem is the following one:

$$(\mathbf{M}\lambda^2+\mathbf{C}_T\lambda+\mathbf{K}_T)\mathbf{u}_0=0 \tag{16}$$

and can be transformed into the phase space by introducing the new eigenvector:

$$\mathbf{X}_0=\begin{Bmatrix}\lambda\mathbf{u}_0\\ \mathbf{u}_0\end{Bmatrix}\in R^{2n}. \tag{17}$$

Therefore the quadratic eigenvalue problem (16) is transformed into the following linear, non-hermitian one:

$$\left(\begin{bmatrix}\mathbf{M} & 0\\ 0 & \mathbf{K}_T\end{bmatrix}-\lambda\begin{bmatrix}0 & \mathbf{M}\\ -\mathbf{M} & -\mathbf{C}_T\end{bmatrix}\right)\begin{Bmatrix}\lambda\mathbf{u}_0\\ \mathbf{u}_0\end{Bmatrix}=0. \tag{18}$$

This equation, assuming regularity and positive definiteness for the mass matrix (i.e., $\det\mathbf{M}\neq 0$ and $\mathbf{M}>0$), can be written:

$$\mathbf{A}_T\mathbf{X}_0=\lambda\mathbf{X}_0 \tag{19}$$

where the matrix $\mathbf{A}_T$ is of order $2n\times 2n$ and is defined by:

$$\mathbf{A}_T=\begin{bmatrix}-\mathbf{M}^{-1}\mathbf{C}_T & -\mathbf{M}^{-1}\mathbf{K}_T\\ \mathbf{I} & 0\end{bmatrix}. \tag{20}$$

The stability behaviour of finite element systems governed by eqn (15) can be studied by examining the nature of the eigenvalues (i.e., they may be complex numbers) of the problem, in the neighbourhood of the current equilibrium solution. Therefore, the eigenvalues $\lambda_k=\alpha_k+i\beta_k$ of (19) at each load step have to be computed by means of a numerical procedure for nonsymmetric matrices and the stability conditions are (e.g., Krätzig, 1993; Gasparini *et al.*, 1995):

(a) if all $\mathrm{Re}(\lambda_k)=\alpha_k$ are negative, the position is asymptotically stable;
(b) if at least one $\mathrm{Re}(\lambda_k)=\alpha_k>0$ exists, the position is unstable. In particular the instability transition occurs *via divergence* if at least one eigenvalue λ_i vanishes, the conjugate λ_j becomes negative real, while the remaining eigenvalues are complex conjugate with negative real parts; or *via flutter* if at least one pair of eigenvalues becomes pure imaginary eigenvalues, while the remaining eigenvalues are complex conjugate with negative real parts;
(c) if some eigenvalues have negative real parts, while the others have zero real parts, the position is weakly stable.

There are the stability assessments of Ljapunov, where the real parts of the characteristic exponents are the well-known Ljapunov exponents.

For undamped systems, usually the stability behaviour is studied by considering the square of the eigenfrequencies of the system defined as $\omega^2=-\lambda^2$. As a consequence the *divergence critical load* is the value of the load to which the smallest square of the eigenfrequencies becomes equal to zero, while the *flutter critical load* is the value of load to which the two smallest eigenvalues approach each other until they coalesce.

The possibility of studying post-critical behaviour, regardless of whether or not the system loses its stability via divergence of flutter, and the ability to characterize the stability regions, i.e., to determine the overall (long-term) response of the system, is associated with the use of the complete nonlinear dynamic analysis of the governing equations, e.g., Thomsen (1993), Kounadis (1994). This global approach, extensively studied by Kounadis in his works for the classical Ziegler's model, can be extended to the analysis of continuous as well as multi-degrees of freedom models, and this will be the subject of a forthcoming paper.

4. BENCHMARK TESTS: UNDAMPED AND DAMPED CRITICAL LOAD

4.1. *Undamped analysis*

In this section some numerical examples drawn from the NAFEMS problems (1990) are developed. The results show the accuracy of the presented three dimensional beam formulation in the stability problems, both for divergence and flutter behaviour.

In particular the NAFEMS problems no. B5, B8, B12a (conservative load) and B12b (nonconservative load), B13, B14 and B18 are studied. For the sake of brevity, the definition of the problems and the results of the analyses are summarised in Figs 2–7. In each figure the geometry of the structure, the deformed geometry of beam mid-axis up to the critical one, the load-displacement diagram of the section in which the load is applied and the load-square of eigenfrequencies curve are shown. Moreover, in each figure the critical load and the mode of instability (i.e., static/divergence of dynamic/flutter) are explicitly marked. Only for the benchmark B8, no critical load is shown, since this structure stays in the stability region for all values of the loads.

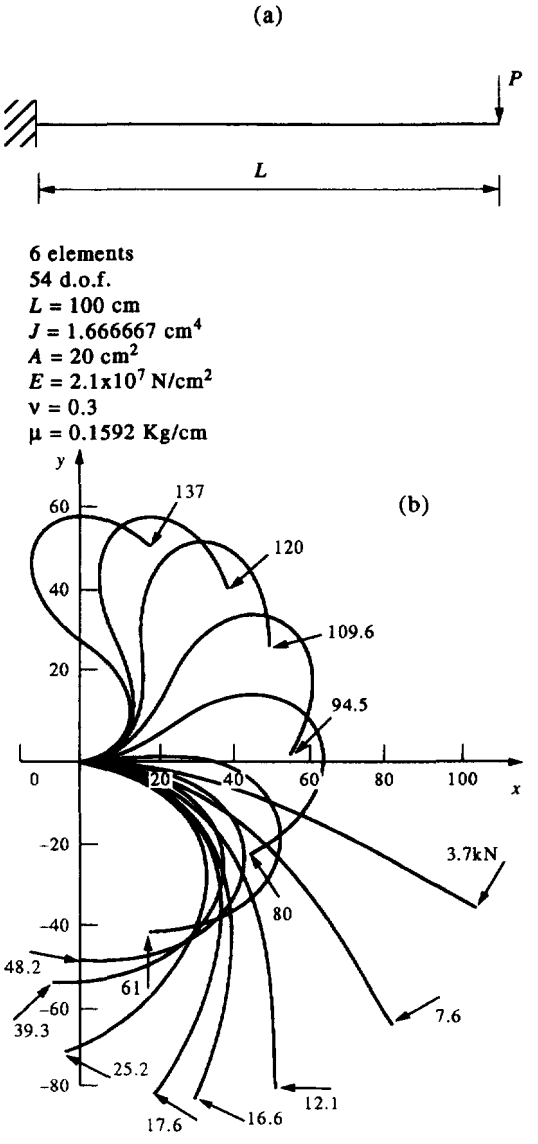

Fig. 2. NAFEMS problems B5: cantilever under follower transverse force (a) geometry; (b) deformed geometry of beam mid-axis; (c) load-displacement diagram of the section of the load application; (d) load–square of eigenfrequencies curve. (*Continued opposite.*)

(c)

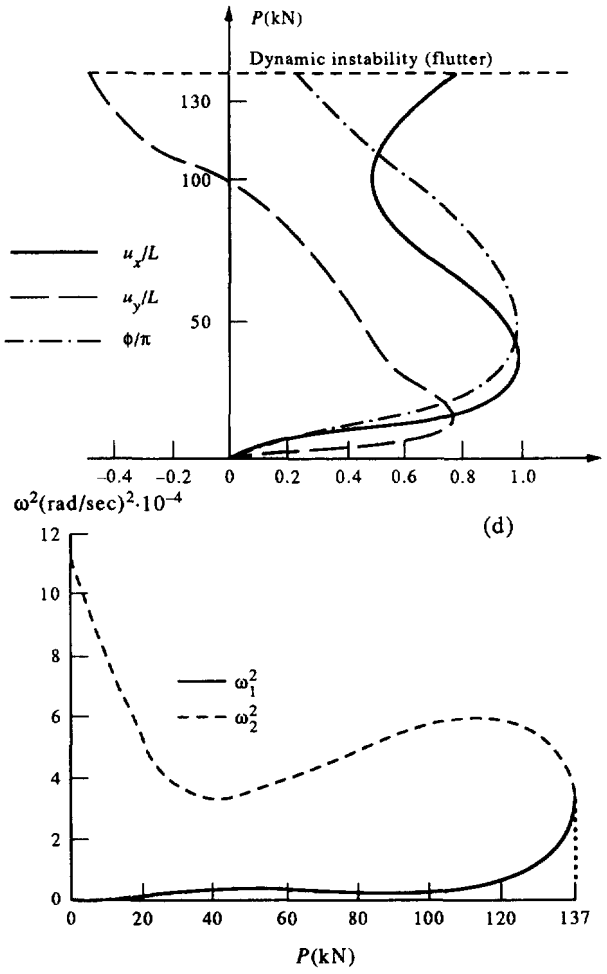

Fig. 2—*Continued.*

A particular attention should be paid to benchmark B18. The results obtained with the developed nonlinear beam theory differ substantially from those published by Argyris and Symeondis (1981a). In particular the deflected shapes after the load value $p = 3$ kN are very different, both quantitatively and qualitatively.

In order to control the correctness of the obtained results, some other tests have been carried out, by using the finite element code ABAQUS and the Simo's approach (Simo *et al.*, 1992) implemented in a numerical procedure. Both these analyses have provided results similar to those shown in Fig. 7a. The disagreement between such results and those reported in Argyris and Symeondis (1981a), may be due to a difference between the scheme and the input data actually used by Argyris and those published in its paper.

Moreover, for the test B18, it has also been noted the behaviour of the diagram load-square of eigenfrequencies (Fig. 7d): in correspondence of the value $p = 5.62$ kN, the two lowest square of eigenfrequencies coincide, showing flutter instability; then the structure remains unstable in flutter region until $p = 9.86$ kN, when a return to stability can be observed. Finally the behaviour becomes definitely unstable via divergence at the value $p = 10.56$ kN.

With reference to the exposed examples, the proposed beam element allows one to study curved structures, as well as rectilinear one, by using a number of degree of freedoms

comparable to that used by some of the published solutions, with almost the same performances. In particular, in order to earn a significant comparison, the vertical and horizontal displacements of the section of the load application for three examples (the curved benchmark tests B13 and B14, and also for the classical rectilinear cantilever under follower transverse force, benchmark test B5) have been calculated for different number of degrees of freedom. This has been done both for the proposed approach and for the ABAQUS's one, while the results of Simo *et al.* (1992), and Argyris and Symeondis (1981a) have been reported only for the cases published in their articles (Tables 1–3). The performances of the four approaches seem to be comparable, even if for the curvilinear structures, the Simo's and Argyris' results are allowable only for a very high number of degrees of freedom, while both the proposed approach and the ABAQUS' one give excellent results even by using a small number of degrees of freedom.

It is worth noting that the aim of this work is to study the stability conditions in terms of type of critical load and effect of damping for the proposed benchmark, while both the

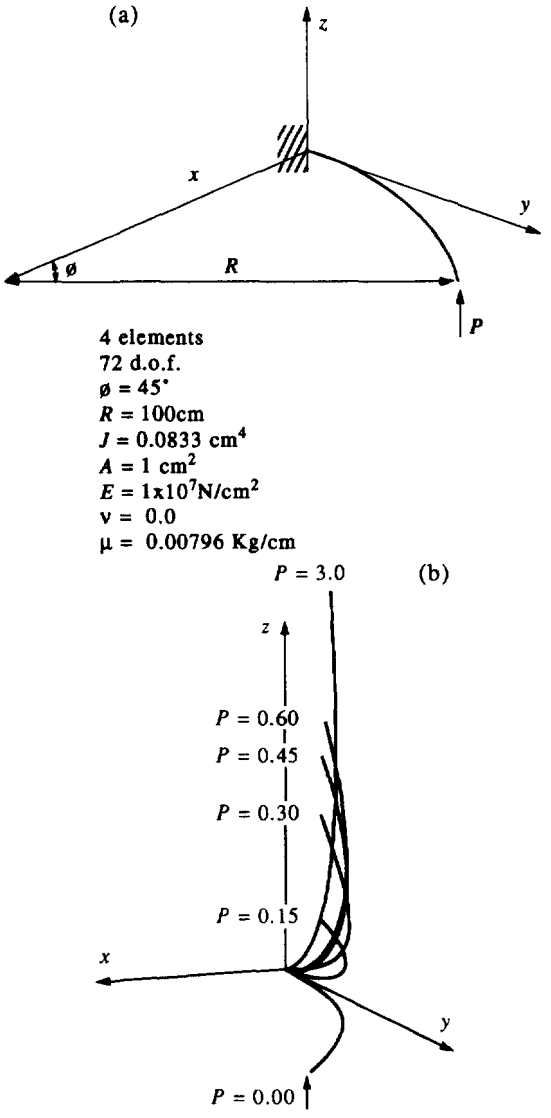

Fig. 3. NAFEMS problems B8: cantilever 45° bend subjected to end load (a) geometry; (b) deformed geometry of beam mid-axis; (c) load-displacement diagram of the section of the load application; (d) load–square of eigenfrequencies curve. (*Continued opposite.*)

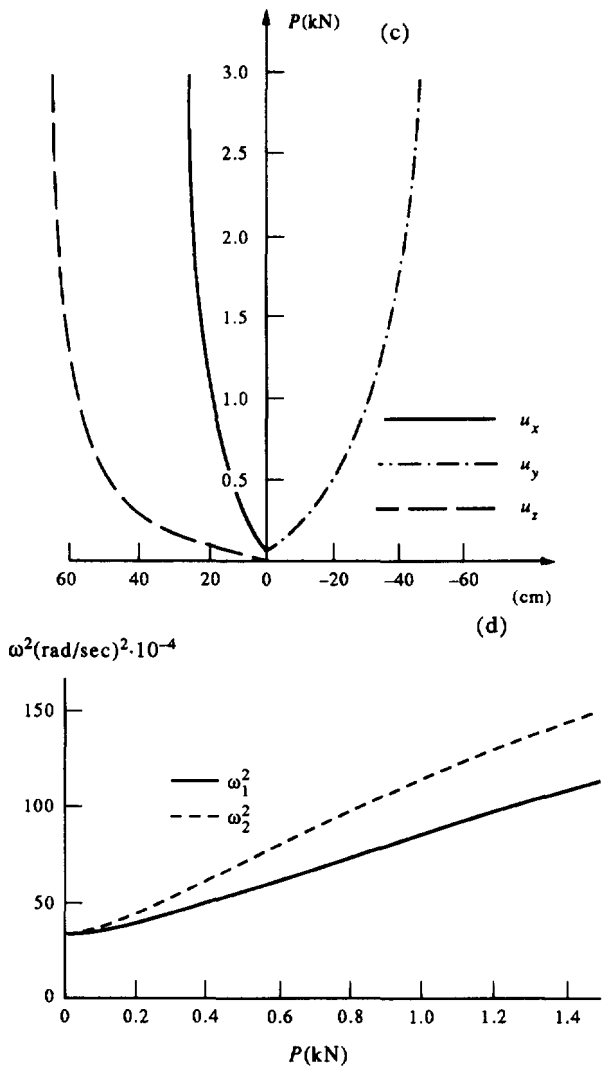

Fig. 3—*Continued.*

Simo's approach and the ABAQUS code are directed to nonlinear analysis of structures, with no reference to stability behaviour, especially under nonconservative loads. For this reason the comparison cannot include an accuracy analysis in the determination of the critical load except for the Argyris and Symeondis results for which the agreement is almost outright.

Table 1. Benchmark B5: comparison between the results obtained with different approaches in terms of displacements (cm) of the section of the load application for a load level $P = 120$ kN

Number of d.o.f.	27/30	36	54	72
Proposed approach	$u_x = -64.2$	$u_x = -64.5$	$u_x = -64.9$	$u_x = -65.2$
	$u_y = 46.1$	$u_y = 42.1$	$u_y = 40.6$	$u_y = 40.6$
Simo's approach	$u_x = -64.3$			
	$u_y = 41.1$			
ABAQUS	$u_x = -64.6$	$u_x = -64.7$	$u_x = -64.9$	$u_x = -64.9$
	$u_y = 40.5$	$u_y = 40.38$	$u_y = 40.4$	$u_y = 40.4$
Argyris approach	$u_x = -61.7$			
	$u_y = 39.2$			

Table 2. Benchmark B13: comparison between the results obtained with different approaches in terms of displacements (cm) of the section of the load application for a load level $P = 5$ kN

Number of d.o.f.	36	54	72	108
Proposed approach	$u_x = -191$ $u_y = 7.97$	$u_x = -187.4$ $u_y = 6.44$	$u_x = -186.6$ $u_y = 6.12$	$u_x = -186.6$ $u_y = 6.13$
Simo's approach				
ABAQUS approach	$u_x = -186.9$ $u_y = 8.47$	$u_x = -186.7$ $u_y = 8.34$	$u_x = -186.7$ $u_y = 8.3$	$u_x = -186.7$ $u_y = 8.2$
Argyris approach				$u_x = -186$ $u_y = 7.8$

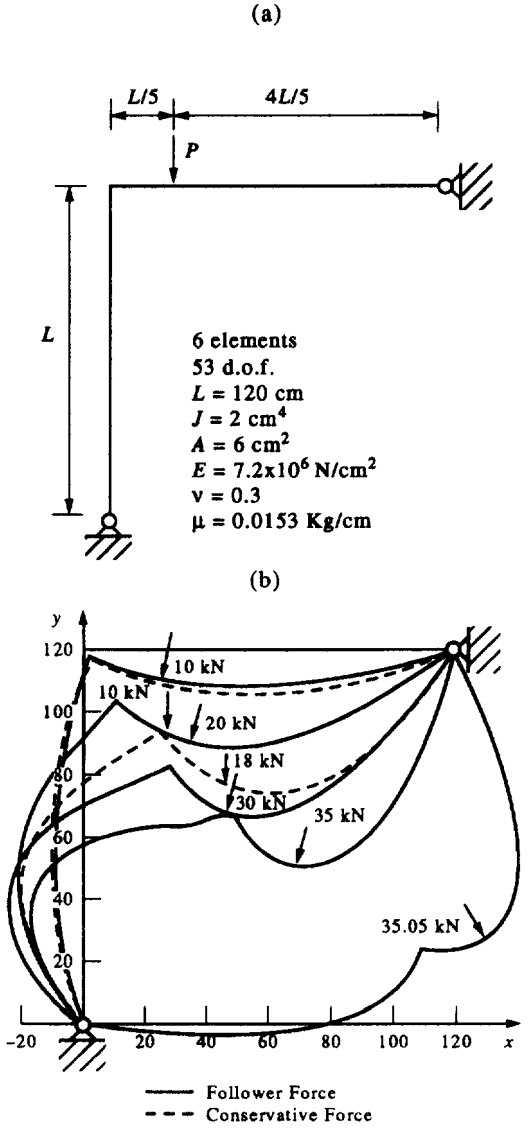

Fig. 4. NAFEMS problems B12a and B12b: Lee's frame (a) geometry; (b) deformed geometry of beam mid-axis; (c) load-displacement diagram of the section of the load application; (d) load–square of eigenfrequencies curve of B12b. (*Continued opposite.*)

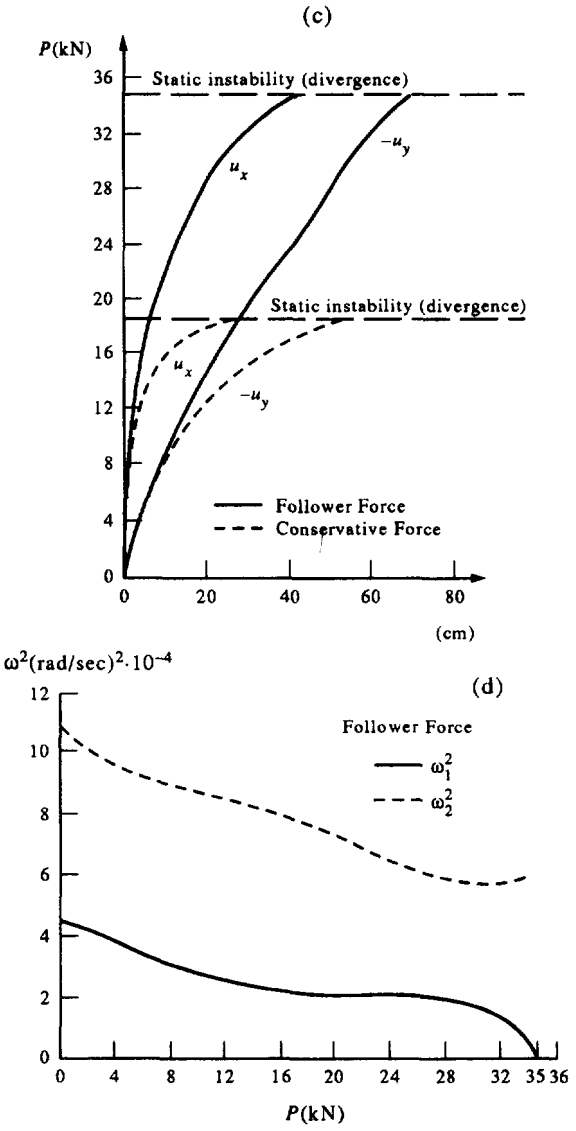

Fig. 4—*Continued.*

Table 3. Benchmark B14: comparison between the results obtained with different approaches in terms of displacements (cm) of the section of the load application for a load level $P = 0.85$ kN

Number of d.o.f.	34	52	70	118
Proposed approach	$u_x = -59$ $u_y = -97$	$u_x = -58.2$ $u_y = -102.13$	$u_x = -58.09$ $u_y = -101.8$	$u_x = -58.1$ $u_y = -101.8$
Simo's approach				
ABAQUS approach	$u_x = -57.52$ $u_y = -100$	$u_x = -58.2$ $u_y = -102.3$	$u_x = -58.27$ $u_y = -102.7$	$u_x = -58$ $u_y = -102.1$
Argyris approach				

Table 4. The influence of variable damping ratio ξ on the critical load value (kN) for three benchmark tests

Damping ratio	Benchmark problem no.		
	B5	B13	B18
$\xi = 0.0$	$P_{flutter} = 137.13$	$P_{flutter} = 5.25$	$P_{flutter} = 5.62$
$\xi = 0.0001$	$P_{flutter} = 127.17$	$P_{flutter} = 4.11$	$P_{flutter} = 4.88$
$\xi = 0.001$	$P_{flutter} = 162.75$	$P_{flutter} = 6.23$	$P_{flutter} = 5.08$
$\xi = 0.005$	$P_{flutter} = 169.63$	$P_{flutter} = 6.43$	$P_{flutter} = 6.50$
$\xi = 0.01$	$P_{flutter} = 169.88$	$P_{flutter} = 6.43$	$P_{flutter} = 10.56$
$\xi = 0.1$	$P_{flutter} = 169.96$	$P_{flutter} = 6.45$	$P_{flutter} = 10.56$

4.2. *Damped analysis*

The effect of damping on the critical flutter load is also investigated, by considering both vanishing and typical damping ratio, and the results are given in Table 4. In particular, Rayleigh-damping has been considered, with variable damping-ratios $\xi_1 = \xi_2 = \xi$ with

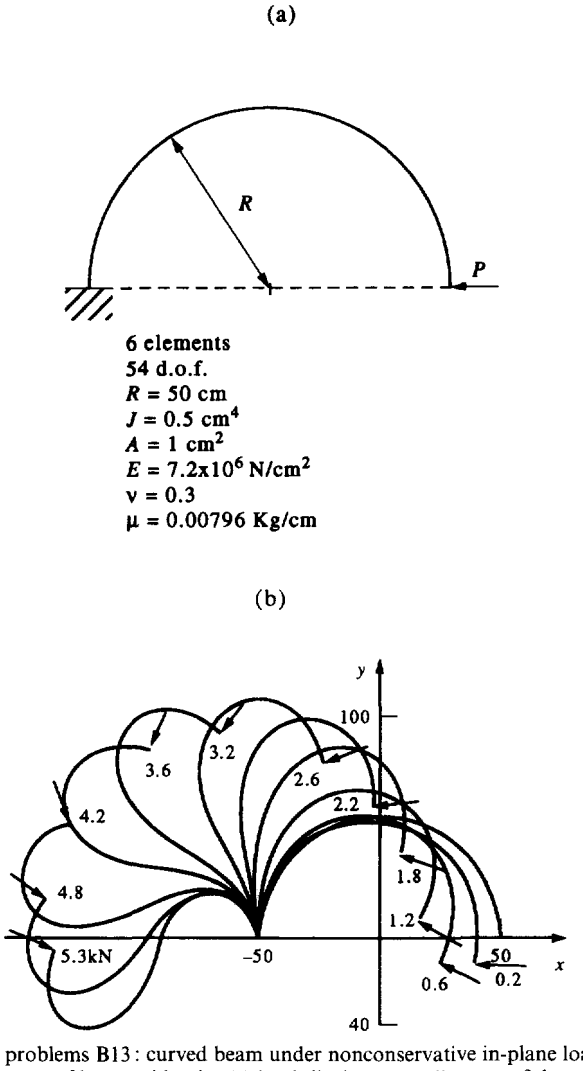

Fig. 5. NAFEMS problems B13: curved beam under nonconservative in-plane load (a) geometry; (b) deformed geometry of beam mid-axis; (c) load-displacement diagram of the section of the load application; (d) load–square of eigenfrequencies curve. (*Continued opposite.*)

(c)

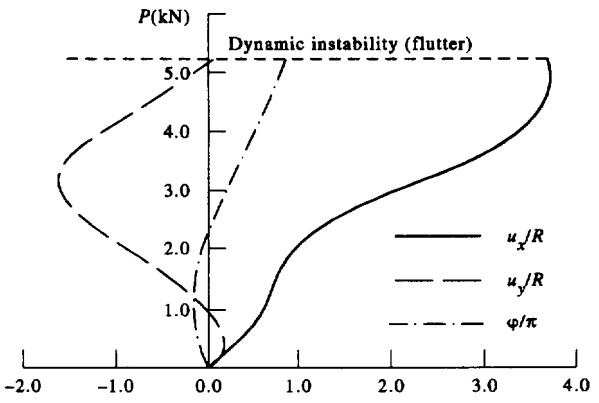

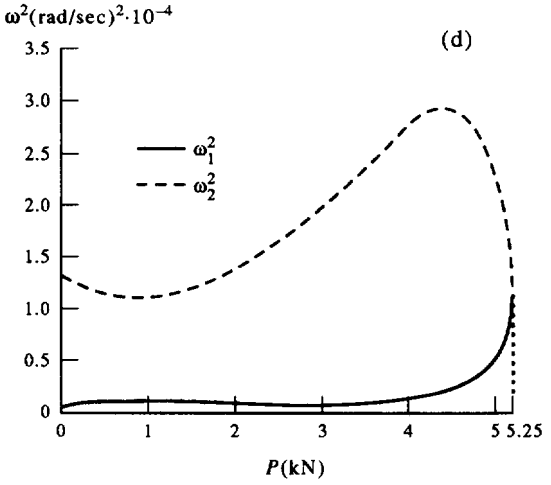

Fig. 5—*Continued.*

respect to the first two eigenfrequencies of the unloaded, stressfree and undeformed structure (Bathe, 1982). The well-known destabilizing effect of vanishing damping, (Bolotin, 1969; Kounadis, 1992 and 1994; Bratus, 1993) i.e., the reduction of the flutter critical load in presence of a small damping ratio, is underlined for all the proposed examples, while a significant value of damping ratio is shown to produce an increase of the value of the flutter critical load.

It is well known that the analyses, in presence of bifurcational systems (i.e., NAFEMS problems no. B8, B12a, B12b, B14), give the same critical (divergence) loads as a static analysis does, regardless of whether or not damping is included.

The results of benchmark B18, also for the damped analysis, require particular attention. Table 4 shows that, as the damping ratio increases, the critical flutter load after an initial decrease, increases until the value $p = 6.8$ kN, in correspondence of $\xi = 0.00584$; then the critical flutter load becomes greater then the value of the divergence critical load $p_{div} = 10.56$ kN (that is not influenced by the presence of damping). Therefore, for $\xi \geqslant 0.00584$, the critical load remains equal to $p = 10.56$ kN and the instability transition occurs via divergence.

The results obtained in presence of uniformly distributed damping along the beam, cannot be considered exhaustive of the problem of stability of damped nonconservative systems. Some more tests, with different values of damping along the beam, as well as a

different way to take into account damping (i.e., the Rayleigh-damping could not be the best one for a nonlinear analysis) need to be developed.

In particular, Ziegler's model may lose its stability via flutter in a region of adjacent equilibrium, e.g., Kounadis (1994). Moreover, by passing from the region of adjacent equilibrium to the region of nonexistence of such equilibrium there may be a loading discontinuity with a flutter load lower than, equal to or higher than the static buckling load, depending on the damping ratio, e.g., Kounadis (1994). These concepts could be extended to multi-degrees of freedom as well as continuous models, but now only the case

(a)

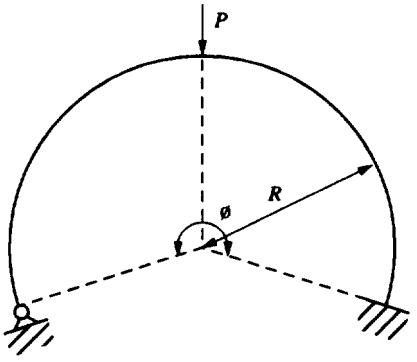

6 elements
52 d.o.f.
ø = 215°
R = 100 cm
J = 0.5 cm^4
A = 6 cm^2
E = 2x10^6 N/cm^2
ν = 0
μ = 0.04776 Kg/cm

(b)

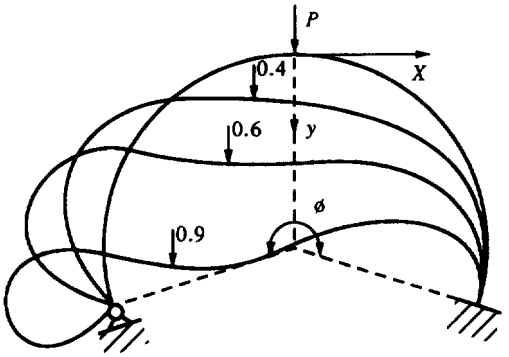

Fig. 6. NAFEMS problems B14: clamped hinged deep circular arch subjected to a point load (a) geometry; (b) deformed geometry of beam mid-axis; (c) load-displacement diagram of the section of the load application; (d) load–square of eigenfrequencies curve. (*Continued opposite.*)

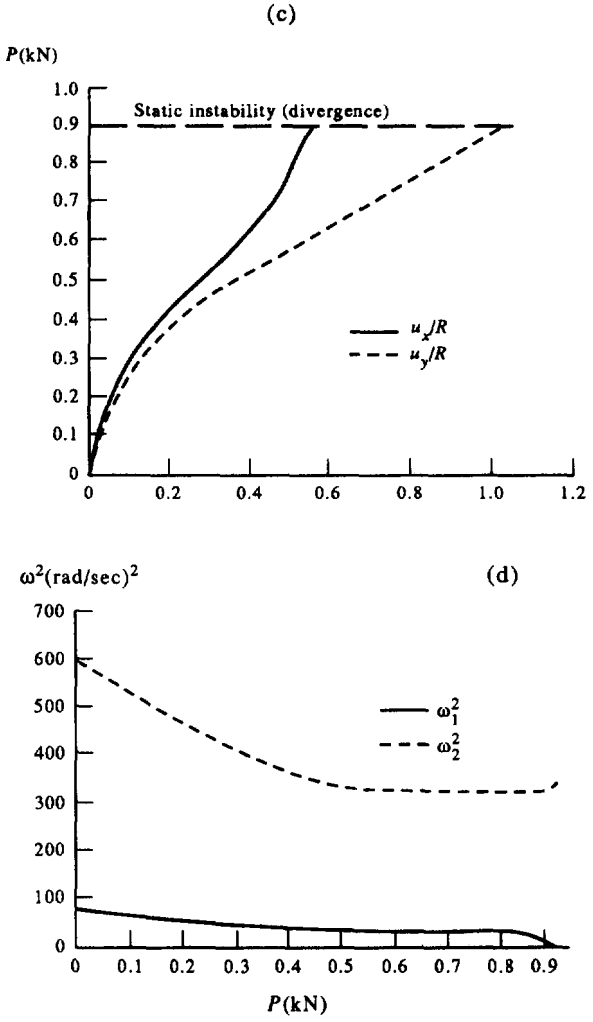

Fig. 6—*Continued.*

of uniformly distributed damping has been considered, for which the flutter critical load still remains equal to or higher than the static buckling load (with reference to the work of Kounadis (1994), this is comparable to the case of equal damping ratios $b_1 = b_2$).

It is worth noting that the definition of benchmark tests for damped nonconservative systems has become more and more imperative within the contest of structural analysis. For this reason the results reported in Table 4 could be considered the first attempt of a standardization of damped nonlinear nonconservative systems, like those reported in the NAFEMS (1990).

5. CONCLUSIONS

A comprehensive study of the stability behaviour of nonlinear nonconservative systems both with and without damping is presented. The most important findings in this research are the following:

- the 3D nonlinear beam element developed here allows to study systems of any geometry by using a limited number of degrees of freedom, even for large curvature;
- the evaluation of the critical load for nonlinear systems subjected to nonconservative load in presence of damping has been carried out for a number of problems drawn from the benchmark list of the NAFEMS publication (1990). Since the absence of damping is not realistic and produces the well-known "destabilization paradoxes" (Bolotin, 1969; Kounadis, 1992 and 1994; Bratus, 1993), here we suggest to define some benchmark tests also for nonlinear damped analyses, with variable damping ratio, and the results here presented could be considered as a starting-point of this proposal.

Acknowledgement—The financial support of the Italian Ministry of Finance is gratefully acknowledged.

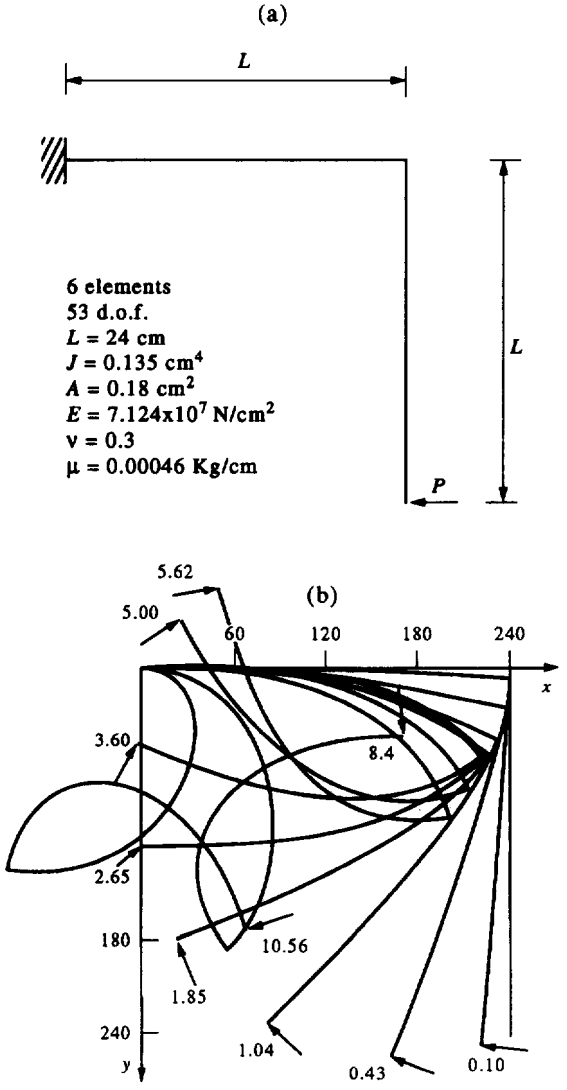

Fig. 7. NAFEMS problems B18: right angled frame under end load (a) geometry; (b) deformed geometry of beam mid-axis; (c) load-displacement diagram of the section of the load application; (d) load–square of eigenfrequencies curve. (*Continued opposite.*)

(c)

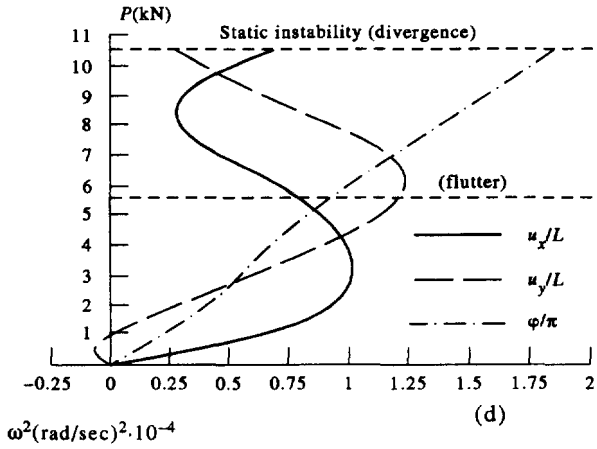

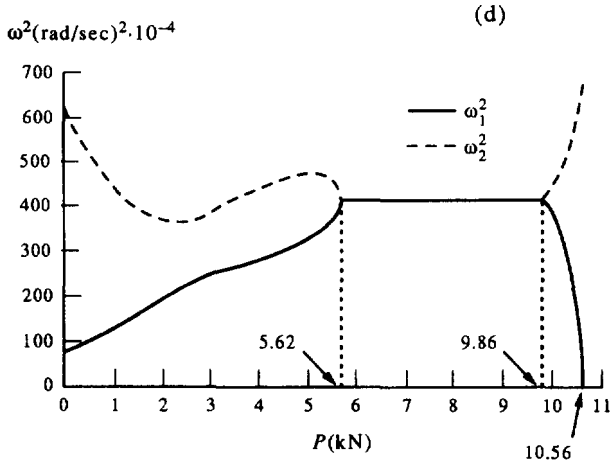

Fig. 7—*Continued.*

REFERENCES

Alliney, S. and Tralli, A. (1984). Extended variational formulations and F.E. models for nonlinear beams under nonconservative loading. *Computers and Methods in Applied Mechanical Engineering* **46,** 177–194.

Argyris, J. H., Straub, K. and Symeondis, S. (1982). Static and dynamic stability of nonlinear elastic systems under nonconservative forces. Natural approach. *Computers and Methods in Applied Mechanical Engineering* **32,** 59–83.

Argyris, J. H. and Symeondis, S. (1981a). A sequel to: nonlinear finite element analysis of elastic systems under nonconservative loading. Natural formulation. Part I Quasistatic problem. *Computers and Methods in Applied Mechanical Engineering* **26,** 377–383.

Argyris, J. H. and Symeondis, S. (1981b). Nonlinear finite element analysis of elastic systems under nonconservative loading. Natural formulation. Part I Quasistatic problem. *Computers and Methods in Applied Mechanical Engineering* **26,** 75–123.

Bathe, K. J. (1982) *Finite Element Procedures in Engineering Analysis*, Prentice-Hall, New Jersey.

Bolotin, V. V. (1965). *Nonconservative Problems of the Theory of Elastic Stability*, Pergamon Press, London.

Bolotin, V. V. and Zhinzher, N.I. (1969). Effects of damping on stability of elastic system subjected to nonconservative forces. *International Journal of Solids and Structures* **5,** 965–989.

Bratus, A. S. (1993). On various cases of instability for elastic nonconservative systems with damping. *International Journal of Solids and Structures* **30,** 3431–3441.

El Naschie, M. S. (1990). *Stress, Stability and Chaos in Structural Engineering. An Energy Approach*, McGraw-Hill, NY.

Gasparini, A. M., Saetta, A. V. and Vitaliani, R. V. (1995). On the stability and instability regions of nonconservative continuous system under partially follower forces. *Computers and Methods in Applied Mechanical Engineering* **124,** 63–78.

NAFEMS (1990). *A Review of Benchmark Problems for Geometric Nonlinear Behaviour of 3D Beams and Shells*, Knowles, N. C.

Kounadis, A. N. (1991). Some new instability aspects for nonconservative systems under follower loads. *International Journal of Mechanical Science* **33,** 297–311.

Kounadis, A. N. (1992). On the paradox of the destabilizing effect of damping in nonconservative systems. *International Journal of Non-Linear Mechanics* **27,** 597–609.
Kounadis, A. N. and Avraam, T. (1993). Global stability analysis of a classical non-conservative system under a follower load. *Journal of Sound and Vibration* **150,** 67–82.
Kounadis, A. N. and Smitses, G. J. (1993). Local (classical) and global bifurcations in non-linear, non-gradient autonomous dissipative structural systems. *Journal of Sound and Vibration*, **160,** 417–432.
Kounadis, A. N. (1994). On the failure of static stability analyses of nonconservative systems in regions of divergence instability. *International Journal of Solids and Structures* **31,** 2099–2120.
Krätzig, W. B., Li, L. Y. and Nawrotzki, P. (1991). Stability conditions for non-conservative dynamical systems. *Computational Mechanics* **8,** 145–151.
Krätzig, W. B. (1993). *Computational Concepts for Kinetic Instability Problems*, Corso CISM, Udine, Italy.
Martini, L. and Vitaliani, R. (1988). On the polynomial convergent formulation of a C^0 isoparametric skew beam element. *Computers and Structures* **29,** 437–449.
Simo, J. C. and Vu-Quoc, L. (1986). Three-dimensional finite-strain rod model. Part II : computational approach. *Computers and Methods of Applied Mechanical Engineering* **X,** 79–116.
Simo, J. C. and Vu-Quoc, L. (1988). On the dynamics in space of rods undergoing large motions—a geometrically exact approach. *Computers and Methods of Applied Mechanical Engineering* **X,** 125–161.
Simo, J. C. and Vu-Quoc, L. (1991). A geometrically exact rod model incorporating shear and torsion-warping deformation. *International Journal of Solids and Structures*, **27,** 371–393.
Surana, K. S and Sorem, R. M. (1989). Geometrically nonlinear formulation for three dimensional curved beam elements with large rotations. *International Journal of Numerical Methods in Engineering* **28,** 43–73.
Thomsen, J. J. (1993). Chaotic dynamics of the partially follower-loaded elastic double-pendulum, *Report no.* 455. Technical University of Denmark.
Vaccaro, G. (1968). *Lezioni di Geometria*, vol. 2, Libreria Eredi Virgilio Veschi, Rome.
Ziegler, H. (1968). *Principles of Structural Stability*, Blaisdell Publ. Co, Toronto.
Zienkiewicz, O. C. and Taylor, R. L. (1989). *The Finite Element Method*, fourth edition, vol. 1.